Structural Engineering and Mechanics, Vol. 45, No.4 (2013) 569-594 569
DOI: http://dx.doi.org/10.12989/sem.2013.45.4.569

Free vibration of tapered arches made of axially functionally graded materials

S. Rajasekaran*

Department of Civil Engineering, PSG College of Technology, Coimbatore, Tamilnadu, India

(Received August 6, 2011, Revised December 4, 2012, Accepted January 26, 2013)

Abstract. The free vibration of axially functionally graded tapered arches including shear deformation and rotatory inertia are studied through solving the governing differential equation of motion. Numerical results are presented for circular, parabolic, catenary, elliptic and sinusoidal arches with hinged-hinged, hinged-clamped and clamped-clamped end restraints. In this study Differential Quadrature element of lowest order (DQEL) or Lagrangian Interpolation technique is applied to solve the problems. Three general taper types for rectangular section are considered. The lowest four natural frequencies are calculated and compared with the published results.

Keywords: free vibration; axially functionally graded material; differential quadrature element method; tapered arch; frequency; boundary condition

1. Introduction

Functionally graded materials (FGM) are multi-phase composites with the volume fraction of phase varying though a direction. FGM was first proposed by materials scientists in the Sendai area in Japan in 1984 (Koizumi 1993, 1997) as thermal barrier material. Since then, these materials have been employed in many engineering application fields such as aircrafts, space vehicles, defense industries, electronics and biomedical sectors. FGM possesses properties that vary gradually through a direction. One advantage of FGM compared to laminated composites is that the material properties continuously vary in thickness or lengthwise directions as opposed to being discontinuous across adjoining layers as they are in laminated composites. For functionally graded arches, gradient variation may be oriented in the cross section / and in the axial direction. For the former, there have been a large number of researches devoted to bending vibration and stability (Malekzadeh 2009, Malekzadeh *et al*. 2010). For axially graded arches similar problem becomes more complicated because of the governing equation with variable coefficients. Many investigators such as Den Hartog (1928), Wolf (1971), Velestos *et al*. (1972), Laura *et al*. (1988) have investigated the vibration of elastic circular arches for various boundary conditions whereas Volterra and Morell (1960), Romanelli and Laura (1972), Wang (1975) investigated the free vibration of elastic arches with various geometries.

*Corresponding author, Professor, E-mail: srs.civ@gapps.psgtech.ac.in

Lee and Wilson (1989) studied the free vibration of arches with variable curvatures. Much research concerned with free vibration of beams are cited by Chidamparam and Leissa (1993). Kang *et al*. (1995) carried out vibration analysis of shear deformable circular arches by the differential quadrature method. Oh *et al.* (1998a, b) arrived at the differential equations governing free in-plane vibrations of circular arches with variable cross sections and solved using numerical technique of Lee and Wilson (1989) and Wilson *et al*. (1984). For non-circular arches with variable cross section, Wang (1975) computed only the fundamental frequency of a clamped parabolic arch by Rayleigh Ritz method. Gutierrez *et al*. (1989) calculated the lowest frequencies in flexure by using polynomial approximation. Maurizi *et al.* (1991, 1993) obtained the lowest frequency of clamped circular arcs of linearly tapered width. Kawakami *et al*. (1995) obtained the free vibration frequencies for in and out of plane vibration of curved members by using discrete Green functions and the numerical integration method. Oh *et al.* (1998a, b, 2000) analyzed for free vibrations of circular arches and non-circular arches with variable cross-sections considering rotatory inertia and shear deformation. Oh *et al.* (2000) conducted experimental investigation for finding frequencies and mode shapes of non circular tapered arches and compared the experimental results with those predicted by theory. Free out-of-plane vibration of a circular arch with uniform cross section are investigated by Tufekci and Dogruer (2006) taking into account the effect of shear and rotatory inertia due to both flexural and torsional vibrations. The governing differential equations were solved exactly using initial value and the results are compared with previous results. Kim and Lee (2008) investigated the role of higher order interpolation functions and consistent stress resultant functions in developing two-node hybrid mixed finite element model including shear deformation for free vibration of arches with rectangular section. Zhao and Kang (2008) derived the governing equations for the free vibration of cable arch using Hamilton's principle and transfer matrix method was used for studying the free vibration of uniform and variable cross sections. In-plane and out-of-plane stability of functionally graded curved beams was first given by Shafiee *et al*. (2006). Malekzadeh and Setoodeh (2009) applied differential quadrature method for moderately thick laminated circular arches with general boundary conditions. The authors used Reissner-Naghdi type shell theory including the effect of shear deformation and rotary inertia. Analysis of in-plane free vibration of functionally graded (FG) thin-to-moderately thick deep circular arches in thermal environment was presented by Malekzadeh *et al*. (2009). The material properties were assumed to be temperature dependent and graded in the thickness direction. The differential quadrature method is adopted to solve thermo elastic equilibrium equations and the equations of motion. Parametric studies were conducted to study the effect of the temperature rise, boundary conditions and material graded index on the natural frequency of FG arches. Malekzadeh (2009) also investigated the in-plane free vibration analysis of FG thick circular arches subjected to initial stress under thermal environment. Malekzadeh (2009, 2010) investigated the in-plane free vibration using elasticity theory for functionally graded (FG) thick circular arches subjected to initial stresses due to the thermal environment. The material properties are assumed to be graded in thickness direction. Malekzadeh *et al*. (2010), Malekzadeh (2010) investigated out-of plane free vibration of functionally graded circular curved beams and assumed that properties are graded in thickness direction. The formulation is based on first order shear deformation theory (FSDT) which includes the effect of shear deformation and rotary inertia. A formulation for the free vibration analysis of functionally graded spatial curved beam is presented by taking into account the effects of thickness and curvature by Yousefi and Rastgoo (2011) based on FSDT. One dimensional model of curved beam with graded properties is developed by incorporating in and out of plane motions to investigate the dynamics and buckling by Piovan *et al.* (2012). They employed Ritz method to obtain the natural frequencies. To the best of author's knowledge, there is no study available in the open literature to show the free vibration of axially functionally graded non circular tapered arches considering shear deformation and rotatory inertia effects.

The main purpose of this paper is to present both the fundamental and some higher free vibration frequencies for axially functionally graded linear elastic circular and non circular arches with variable cross section for different support conditions. The equations taking into account both shear deformation and rotary inertia given by Oh *et al.* (1998a, 1998b, 2000) and Huang *et al*. (1998) are considered in this paper. The equations were solved by Oh *et al.* (1998, 2000) using Runge-Kutta method and by Huang *et al*. (1998) using Frobenius method. Romanelli and Laura (1972) obtained the fundamental frequency of non-circular elastic hinged arcs. In this paper the equations are solved numerically by using Differential quadrature method of lowest order (DQEL) (Lagrangian interpolation technique) for arches of circular, parabolic, catenary, elliptic and sinusoidal geometries with non uniform cross section with hinged-hinged, hinged-clamped and clamped –clamped boundary conditions. The lowest four frequencies in terms of arch rise to span length ratio ($f = h/s$ where h is the height of the arch and 's' span), slenderness ratio $S = s/\sqrt{I_c / A_c}$ and section ratio $n = I_s/I_c$ are arrived at and the results are compared with already published results

2. Mathematical formulation

Consider a symmetric non-circular arch with non-uniform cross section as shown in Fig. 1(a). its span length, rise, semi subtended angle and the shape of the middle surface are 's, h, θ, and $y(x)$ respectively. It is to be noted that the left support of the arch is taken as origin and x and y are the coordinates in the positive directions. The radius of curvature 'r' of the arch is a function of coordinate α (angle between normal of the arch at any section to the horizontal measured in clockwise direction). Fig. 1(a) also shows the direction of radial and tangential displacements and positive rotation angle of the cross section at point 'α' of the arch as w, v and ψ in the positive directions. A small element shown in Fig. 1(b) gives the positive directions for the stress resultants : viz: - P – the axial forces; V – the shear forces; M- the bending moments. The radial and tangential inertia forces are denoted by F_r, F_t respectively and the rotatory inertial couple as T. The dynamic equilibrium equations of the element as given by Oh *et al*. (1998, 2000, 1998) and Huang *et al*. (1998) are

$$\frac{dP}{d\alpha} + V + r F_t = 0 \tag{1a}$$

$$\frac{dV}{d\alpha} - P + r F_r = 0 \tag{1b}$$

$$\frac{dM}{d\alpha} - r V - r\ T = 0 \tag{1c}$$

where

$$F_t = \rho A \omega^2 v; \quad F_r = \rho A \omega^2 w; \quad T = \rho I \omega^2 \psi \tag{2}$$

ρ denotes the mass density of the material.

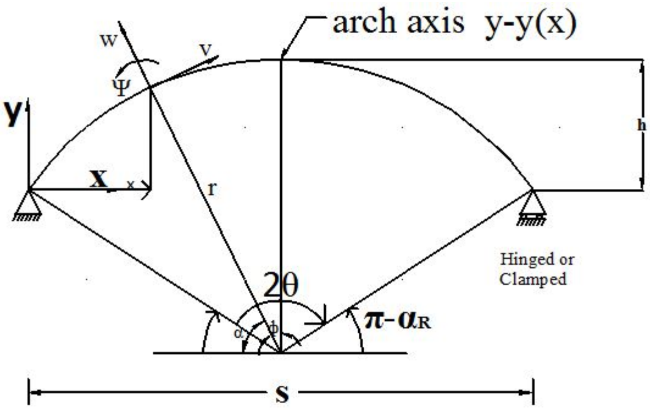

Fig. 1(a) Arch geometry

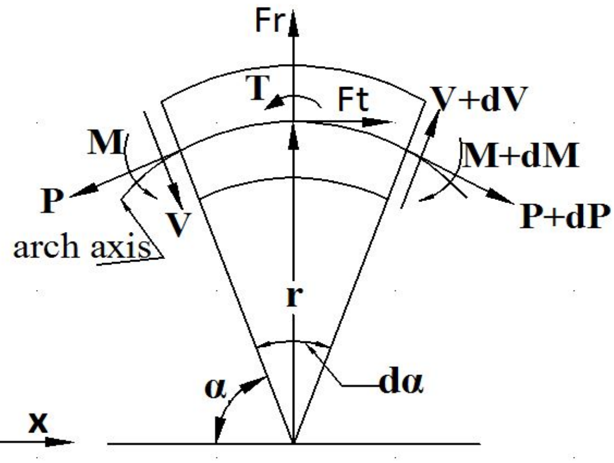

Fig. 1(b) Equilibrium of an arch element

Since in Timoshenko beam theory, plane sections still remain plane but are no longer normal to the longitudinal axis. The difference between the normal to the longitudinal axis and the plane section rotation is the shear deformation. It is assumed constant shear stresses on the cross section which, however, is not true in actual situations. Hence a shear correction factor *k* of the cross section is always introduced.

Hence the rotation of the tangent to the centroidal axis may be given by

$$\chi = \psi + \beta = \frac{1}{r}\left(\frac{dw}{d\alpha} - v\right) \tag{3}$$

or shearing deformation β is given by

$$\beta = \frac{1}{r}\left(\frac{dw}{d\alpha} - v - r\psi\right) \tag{4}$$

Using strength of materials, the bending moment , normal force and shear force are given by Borg and Gennaro (1959).

$$M = -\frac{EI}{r}\frac{d\psi}{d\alpha} \tag{5}$$

$$P = \frac{EA}{r}\left(\frac{dv}{d\alpha} + w\right) + \frac{EI}{r^2}\frac{d\psi}{d\alpha} = \frac{EA}{r}\left(\frac{dv}{d\alpha} + w\right) - \frac{M}{r} \tag{6}$$

$$V = k\,A\,G\,\beta = \frac{kAG}{r}\left(\frac{dw}{d\alpha} - v - r\psi\right) = \frac{\mu\,A\,E}{r}\left(\frac{dw}{d\alpha} - v - r\psi\right) \tag{7}$$

Some authors like Henrych (1989), Friedman and Kosmatka (1998) and Shahba *et al*. (2012) have not considered M/r in the equation of P (Eq. (6)) since they assumed that centroidal axis and neutral axis are the same. Actually, neutral axis is displaced from the centroidal axis resulting in hyperbolic stress distribution (Boresi *et al*. 1978) instead of linear stress distribution. This type of formulation is more accurate for short deep beams. For the arches considered in this paper it is immaterial whether we consider M/r or not.

In Eq. 7 $\mu = kG/E$ and I is the moment of Inertia of the arch section at any section and A is the area and k is the shear correction factor and G is the shear modulus. In all the numerical examples nod-dimensional i^{th} frequency parameter is computed as

$$C_i = \omega_i\, s^2\sqrt{\frac{A_c\,\rho_c}{I_c\,E_c}} = \omega_i\, S\, s\sqrt{\frac{\rho_c}{E_c}} \tag{8a}$$

where

$$S = \frac{s}{\sqrt{\frac{I_c}{A_c}}} \tag{8b}$$

ρ_c, E_c, A_c, I_c are the mass density, Young's modulus, area of the cross section and moment of inertia of the cross section at the crown and when the subscript is replaced by s they denote the corresponding values at the support.

2.1 Geometry of the arch

Even though the geometric functions such as shape of the arch, radius of curvature and the opening angle for practical curves are given in may text books (Lockwood 1961, Lawrence 1972) and in many research papers (Oh *et al*. 1998a, 1998b, 2000), they are illustrated briefly here for completeness. In the following, we consider symmetric arches and the origin is assumed to be at the left support.

2.1.1 Circular arch

To determine the geometry of the arch, two values viz: - height (h) and span length (s) are needed. Then the equation of the arch is given by

$$\left(x-\left(\frac{s}{2}\right)\right)^2+(y+r-h)^2=r^2 \qquad 0\le x\le s \tag{9}$$

The arch opening angle 2θ is given by

$$2\theta = 2\tan^{-1}\left(\frac{s}{2(r-h)}\right) \tag{10}$$

2.1.2 Parabolic arch

Similar to circular arch, to arrive at the geometry of a parabolic arch, we need the height (*h*) and span length (*s*). The equation of the arch is given by

$$y=\frac{4h}{s^2}x(s-x) \qquad 0\le x\le s \tag{11}$$

The arch opening angle 2θ is given by

$$2\theta = 2\tan^{-1}\left(\left.\frac{dy}{dx}\right|_{x=0}\right) \tag{12}$$

$$2\theta = 2\tan^{-1}\left(\frac{4h}{s}\right) \tag{13}$$

2.1.3 Catenary arch

If the height (*h*) and span length (*s*) are given, one has to solve the following nonlinear equation to arrive at the radius of curvature r_c at the crown as

$$-r_c\cosh\left(\frac{s}{2r_c}\right)+h+r_c=0 \tag{14}$$

The equation of the catenary arch is given by

$$y=-r_c\cosh\left(\frac{(2x-s)}{2r_c}\right)+h+r_c \qquad 0\le x\le s \tag{15}$$

The arch opening angle 2θ is given by

$$2\theta = 2\tan^{-1}\left(\sinh\left(\frac{s}{2r_c}\right)\right) \tag{16}$$

2.1.4 Elliptic arch

For elliptic arch in addition to span (*s)* height of the arch (*h*) and another parameter δ has to be given such that semi major axis of the arch a is given by

$$a = \frac{s}{2} + s\delta \tag{17}$$

Then semi minor axis b can be calculated as

$$b = \frac{h}{1 - \sqrt{1 - 0.25\left(\frac{s}{a}\right)^2}} \tag{18}$$

The equation of the elliptic arch is given by

$$\frac{(x + s\delta - a)^2}{a^2} + \frac{(y + b - h)^2}{b^2} = 1 \qquad 0 \le x \le s \tag{19}$$

Finding $\left.\frac{dy}{dx}\right|_{x=0}$ will give the opening angle of the elliptic arch as

$$2\theta = 2\tan^{-1}\left(\left.\frac{dy}{dx}\right|_{x=0}\right) \tag{20}$$

2.1.5 Sinusoidal arch

For sinusoidal arch in addition to span (s), height of the arch (h) another parameter δ has to be given such that

$$L = s + 2s\delta \tag{21}$$

The equation of sinusoidal arch is given as

$$y = h\left(1 - \frac{\left(1 - \sin \pi\left(\frac{x + s\delta}{L}\right)\right)}{\left(1 - \sin\frac{\pi s\delta}{L}\right)}\right) \tag{22}$$

The opening angle of the arch 2θ may be calculated as

$$2\theta = 2\tan^{-1}\left(\left.\frac{dy}{dx}\right|_{x=0}\right) \tag{23}$$

For all the arches except circular arch, radius of curvature ‘r’ is calculated as

$$r = \frac{\left(1 + \left(\frac{dy}{dx}\right)^2\right)^{3/2}}{\frac{d^2y}{dx^2}} \tag{24}$$

2.1.6 Variation of I and A

The area and moment of inertia of the arch cross section at a section *A* and *I* are written in terms of their corresponding values at the crown. Out of two classes of arched members, there are two forms viz; prime and quadratic. Quadratic forms (Leontovich 1969) are adopted in practice. Since the quadratic arch is considered more economical in bridge construction and hence it is adopted here.

The formulation given above can take into account any variation of area and moment of inertia of the sections. In order to compare the results of present analysis with that of Oh *et al*. (1998a, b), we consider the variation *A* and *I* as given by Oh *et al.* (1998a, b) as

$$A = A_c \Gamma; \quad I = I_c\, \Omega \tag{25}$$

where Γ and Ω are functions of a single variable α given by

$$\Omega = \frac{1}{\sin\alpha(1+\kappa\cos^2\alpha)} \tag{26}$$

where

$$\kappa = \frac{1}{\sin^2\theta}\left\{\frac{1}{n\cos\theta} - 1\right\} \tag{27}$$

(a) depth taper: - In this case $I = \Omega\, I_c$ or $d = \Omega^{1/3} d_c$ and hence $A = \Omega^{1/3} A_c = \Gamma A_c$ or $\Gamma = \Omega^{1/3}$.

(b) breadth taper: In this case $I = \Omega\, I_c$ or $b = \Omega\, b_c$ and hence $A = \Omega\, A_c = \Gamma A_c$ or $\Gamma = \Omega$

(c) square taper: (similar to diameter taper of a circular section) $I = \Omega\, I_c$ or $d = \Omega^{1/4} d_c$ and hence $A = \Omega^{1/2} A_c = \Gamma A_c$ and hence $\Gamma = \Omega^{1/2}$

In general Γ is given by

$$\Gamma = \Omega^p \tag{28}$$

where p = 0.3333, 1.0 and 0.5 for depth, breadth and square (both) taper respectively (Gupta 1985). And the section ratio '*n*' is given by

$$n = \frac{I_s}{I_c} \tag{29}$$

where I_s, I_c are the moments of inertia of the arch sections at the support and crown respectively.

3. Variation of material properties such as E (Young's modulus), G (Shear modulus) and ρ (mass density)

Consider a solid functionally graded symmetric arch having spatially continuously varying material property along certain direction and in our case arch axis direction. In general, spatial varying material property *Y* including Young's modulus, shear modulus and mass density may be expressed as

$$Y = \sum_{j=1}^{n} Y_j V_j \tag{30}$$

where Y_j, V_j are the material property and volume fraction of j[th] constitutive phase. For all V_j the following equation must be satisfied.

$$\sum_{j=1}^{n} V_j = 1 \qquad 0 \le V_j \le 1 \tag{31}$$

Consider a symmetric arch made of an axially functionally graded material whose constituents are Zirconia ZrO_2 (E_z = 200 GPa, $\gamma_z = 5700 kg/m^3$) and Aluminum Al (E_a = 70GPa; $\gamma_z = 2702 kg/m^3$). The volume fraction of Zirconia is given as

$$V_z = (\frac{(e^{\eta\xi} - 1)}{(e^{\eta} - 1)}; \; V_a = 1 - V_z \tag{32}$$

The distribution of modulus of elasticity and the mass density are assumed to follow an exponential relation as (Shahba *et al*. 2011, Shahba and Rajasekaran 2011)

$$T = T_a + (T_z - T_a)(\frac{(e^{\eta\xi} - 1)}{(e^{\eta} - 1)} \quad if \;\; \eta \ne 0 \tag{33}$$

$$T = T_a + (T_z - T_a)\xi \qquad if \;\; \eta = 0 \tag{34}$$

where

$$\xi = \frac{\phi}{\theta} \tag{35}$$

and η is the material non- homogeneity parameter.

To compare the values with Oh *et al.* (1998a, b, 2000), Poisson's ratio and *G* are calculated according to the value of μ. It is assumed that the arch is aluminum rich at $\xi = 0$ (at crown) and Zirconia rich at $\xi = 1$ (at support). The variation of modulus of elasticity along half of the arch is plotted for different non-homogeneity parameter η in Fig. 2. It is observed from Fig. 2 that the percentage content of aluminum is increased as higher values of non-homogeneity parameter are considered. Consequently, the stiffness and weight of beam are reduced.

4. Differential quadrature element method of lowest order

In addition to Finite element, Finite difference, Differential transformation methods, Differential quadrature method (DQM) is yet another efficient method for solving differential equations. DQM was introduced by Bellman and Casti (1971). The basic concept of the method is that derivative of a function at a given point can be approximated as a weighted sum of function values at all of the sampling points in the domain of that variable. Hence it is possible to reduce differential equations into a set of algebraic equations using the above approximation and boundary condition applied. The accuracy of the method depends on the number of sampling

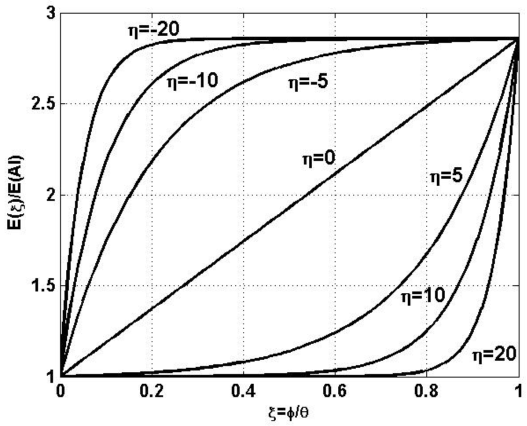

Fig. 2 Variation of E along half of the arch according to material parameter

points used. Since the introduction of the method, application to various engineering problems has been investigated and their success has shown the potential of the method as attractive numerical technique (Bert *et al*. 1993, Bert *et al*. 1994, Rajasekaran 2007, 2008, Shu 2000). In this paper, Differential quadrature element of lowest order (DQEL) or simply Lagrangian interpolation technique has been applied to solve free vibration of any tapered arch of axially functionally graded material including shear deformation and rotary inertia.

Lagrangian Interpolation Method (Schilling and Harris 2000)

⅄ This interpolation technique is applied if the given points in an element may or may not be equally spaced. But in this paper equally spaced sample points are considered.

⅄ The polynomial is an approximation to the function $y = f(x)$, which coincides with the polynomial at (x_i, y_i). Assuming 'n' sampling points.

$$\phi_k = p\prod_{\substack{i=1 \\ i\neq k}}^{n}(x - x_i) \tag{36}$$

The constants p can be evaluated and the function ϕ_k is given by,

$$\phi_k = \frac{\prod_{\substack{i=1 \\ i\neq k}}^{n}(x - x_i)}{\prod_{\substack{i=1 \\ i\neq k}}^{n}(x_k - x_i)} \tag{37}$$

If the subtended angle of the arch element is $L = 2\theta / ne$ (*ne* = no of elements) and defining $\xi = \phi / L$, the shape function is given by

$$N_k = \frac{\prod_{i=1,\ i\neq k}^{n} (\xi - \xi_i)}{\prod_{i=1,\ i\neq k}^{n} (\xi_k - \xi_i)} \tag{38}$$

Using the shape functions one can obtain the values of 'y' at any point as

$$y = < N_1 \quad N_2 \quad N_3 \quad ..... \quad N_n > \{\underline{y}\} \tag{39}$$

where $\underline{\mathbf{y}}$ are the function values at the sampling points.

The first order differential at various sampling points is given as

$$\underset{n\times 1}{\begin{Bmatrix} \left.\frac{dy}{dx}\right|_1 \\ \left.\frac{dy}{dx}\right|_2 \\ \vdots \\ \left.\frac{dy}{dx}\right|_n \end{Bmatrix}} = \frac{1}{L} \underset{n\times 1}{\begin{Bmatrix} \left.\frac{dy}{d\xi}\right|_1 \\ \left.\frac{dy}{d\xi}\right|_2 \\ \vdots \\ \left.\frac{dy}{d\xi}\right|_n \end{Bmatrix}} = \frac{1}{L} \underset{n\times n}{\begin{bmatrix} N_{1,\xi}|_1 & N_{2,\xi}|_1 & . & . & N_{n,\xi}|_1 \\ N_{1,\xi}|_2 & N_{2,\xi}|_2 & . & . & N_{n,\xi}|_2 \\ . & . & . & . & . \\ . & . & . & . & . \\ N_{1,\xi}|_n & N_{2,\xi}|_n & . & . & N_{n,\xi}|_n \end{bmatrix}} \underset{n\times 1}{\begin{Bmatrix} y_1 \\ y_2 \\ . \\ . \\ y_n \end{Bmatrix}} = [c]\{\underline{y}\} \tag{40}$$

where [c] is a *nxn* matrix of first order defined as *c*(*n,n*,1) or simply **c,** '*n*' being the number of sampling points taken as equally spaced and 1 denotes the result of first order differentiation. In this paper, we use only first order differential of Lagrangian interpolation functions and hence the name of the method.

5. Free vibration of axially functionally graded symmetric arches

The equilibrium and constitutive law for the arch element may be written in matrix form as

$$\begin{bmatrix} \nabla & 1 & 0 & 0 & 0 & 0 \\ -1 & \nabla & 0 & 0 & 0 & 0 \\ 0 & -r & \nabla & 0 & 0 & 0 \\ 0 & 0 & \frac{r}{EI} & \nabla & 0 & 0 \\ -\frac{r}{EA} & 0 & -\frac{1}{EA} & 0 & \nabla & 1 \\ 0 & -\frac{r}{kAG} & 0 & -r & -1 & \nabla \end{bmatrix} \begin{Bmatrix} P \\ V \\ M \\ \psi \\ v \\ w \end{Bmatrix} = \omega^2 \begin{bmatrix} 0 & 0 & 0 & 0 & -rA\rho & 0 \\ 0 & 0 & 0 & 0 & 0 & -rA\rho \\ 0 & 0 & 0 & rI\rho & 0 & 0 \\ 0 & 0 & 0 & 0 & 0 & 0 \\ 0 & 0 & 0 & 0 & 0 & 0 \\ 0 & 0 & 0 & 0 & 0 & 0 \end{bmatrix} \begin{Bmatrix} P \\ V \\ M \\ \psi \\ v \\ w \end{Bmatrix}$$

(41)

Denoting $\nabla = \frac{d}{d\alpha}$ (α denotes the inclination of radius of curvature r with x axis) in Eq. 41, $\nabla\mathbf{P}, \nabla\mathbf{V}, \nabla\mathbf{M}, \nabla\boldsymbol{\psi}, \nabla\mathbf{v}$ **and** $\nabla\mathbf{w}$ etc can be written using Lagrangian interpolation polynomial as

$$\nabla P_i = \mathbf{c}\,\underline{\mathbf{P}}_{\mathbf{i}};\nabla V_i = \mathbf{c}\underline{\mathbf{V}}_{\mathbf{i}};\nabla M_i = \mathbf{c}\,\underline{\mathbf{M}}_{\mathbf{i}};\nabla\psi_i = \mathbf{c}\,\underline{\boldsymbol{\psi}}_{\mathbf{i}};\nabla v_i = \mathbf{c}\,\underline{\mathbf{v}}_{\mathbf{i}};\nabla w_i = \mathbf{c}\,\underline{\mathbf{w}}_{\mathbf{i}} \tag{42}$$

where $\{\underline{P}\}_i, \{\underline{V}\}_i, \{\underline{M}\}_i$ are the stress resultants at the sampling points and $\underline{\{\psi\}_i}$, $\underline{\{v\}_i}$ *and* $\underline{\{w\}_i}$ are the rotation, tangential and radial displacements at the sampling points of the ith element as

$$\begin{aligned}
&\underline{\mathbf{P}}_i = \{P(i,1)\ P(i,2)\cdots P(i,n)\}^T;\ \underline{\mathbf{V}}_{\mathbf{i}} = \{V(i,1)\ V(i,2)\cdots V(i,n)\}^T\\
&\underline{\mathbf{M}}_{\mathbf{i}} = \{M(i,1)\ M(i,2)\cdots M(i,n)\}^T;\ \underline{\boldsymbol{\psi}}_{\mathbf{i}} = \{\psi(i,1)\ \psi(i,2)\cdots\psi(i,n)\}^T\\
&\underline{\mathbf{v}}_{\mathbf{i}} = \{v(i,1)\ v(i,2)\cdots v(i,n)\}^T;\ \ \underline{\mathbf{w}}_{\mathbf{i}} = \{w(i,1)\ w(i,2)\cdots w(i,n)\}^T
\end{aligned} \tag{43}$$

Hence $\nabla P, \nabla V, \nabla M, \nabla\psi, \nabla v, \nabla w$ at any point are given by Eq. 42 where ∇ is replaced by **c**, **1/EI** is the diagonal matrices consisting of the values of inverse of flexural rigidities at the sampling points. For the axially functionally graded tapered arch, the variation of Young's modulus *E(x)*, mass density, $\rho(x)$, area, $A(x)$ and Moment of Inertia, *I(x)* at sampling points will be known. Hence for an element the differential system is written as

$$\begin{bmatrix}
[c] & [I] & [0] & [0] & [0] & [0]\\
-[I] & [c] & [0] & [0] & [0] & [0]\\
[0] & -[r] & [c] & [0] & [0] & [0]\\
[0] & [0] & [\frac{r}{EI}] & [c] & [0] & [0]\\
-[\frac{r}{EA}] & [0] & -[\frac{I}{EA}] & [0] & [c] & [I]\\
[0] & -[\frac{r}{kAG}] & [0] & -[r] & -[I] & [c]
\end{bmatrix}
\begin{Bmatrix}\{\underline{P}\}\\ \{\underline{V}\}\\ \{\underline{M}\}\\ \{\underline{\psi}\}\\ \{\underline{v}\}\\ \{\underline{w}\}\end{Bmatrix}$$

$$= \omega^2 \begin{bmatrix}
[0] & [0] & [0] & [0] & -[\rho Ar] & [0]\\
[0] & [0] & [0] & [0] & [0] & -[\rho Ar]\\
[0] & [0] & [0] & [\rho Ir] & [0] & [0]\\
[0] & [0] & [0] & [0] & [0] & [0]\\
[0] & [0] & [0] & [0] & [0] & [0]\\
[0] & [0] & [0] & [0] & [0] & [0]
\end{bmatrix}
\begin{Bmatrix}\{\underline{P}\}\\ \{\underline{V}\}\\ \{\underline{M}\}\\ \{\underline{\psi}\}\\ \{\underline{v}\}\\ \{\underline{w}\}\end{Bmatrix} \tag{44}$$

where **I** is the identity matrix and *E(x)I(x)* is the flexural rigidity at the sampling point. In Eq. 44, *G(x)* denotes the shear modulus and *k*, the shear correction factor and for rectangular section it is taken as 0.833. The value of shear modulus is taken so as to satisfy $\mu = kG/E$. For the *i*th element this can be written as

$$\underset{nt\times nt}{\mathbf{D_i}}\ \underset{nt\times 1}{\mathbf{q_i}} = \omega^2\ \underset{nt\times nt}{\mathbf{m_i}}\ \underset{nt\times 1}{\mathbf{q_i}} \tag{45}$$

where $\mathbf{q_i}$ is given by

$$\mathbf{q_i} = \begin{Bmatrix} \underline{\mathbf{P}}_\mathbf{i} \\ \underline{\mathbf{V}}_\mathbf{i} \\ \underline{\mathbf{M}}_\mathbf{i} \\ \underline{\mathbf{\Psi}}_\mathbf{i} \\ \underline{\mathbf{v}}_\mathbf{i} \\ \underline{\mathbf{w}}_\mathbf{i} \end{Bmatrix} \tag{46}$$

At each node one has to find three stress resultants and three deformations and in total there are six unknowns. If there are '*n*' sampling points total number of unknowns for each element will be $nt = 6\times \mathrm{n}$. Usually *n* is taken as 11 (with 10 equal divisions) and hence the total number of unknowns for each element will be $nt = 11\times 6 = 66$. If the arch is idealized into *ne* = 12 elements, the differential system is given by

$$\underset{(66\times 12)\times(66\times 12)}{\begin{bmatrix} \mathbf{D_1} & & & & & \\ & \mathbf{D_2} & & & & \\ & & \mathbf{D_3} & & & \\ & & & & & \\ & & & & \mathbf{D_{11}} & \\ & & & & & \mathbf{D_{12}} \end{bmatrix}} \underset{792\times 1}{\begin{Bmatrix} \mathbf{q_1} \\ \mathbf{q_2} \\ \mathbf{q_3} \\ - \\ - \\ \mathbf{q_{12}} \end{Bmatrix}} = \boldsymbol{\omega}^2 \underset{792\times 792}{\begin{bmatrix} \mathbf{m_1} & & & & & \\ & \mathbf{m_2} & & & & \\ & & \mathbf{m_3} & & & \\ & & & & & \\ & & & & \mathbf{m_{11}} & \\ & & & & & \mathbf{m_{12}} \end{bmatrix}} \begin{Bmatrix} \mathbf{q_1} \\ \mathbf{q_2} \\ \mathbf{q_3} \\ - \\ - \\ \mathbf{q_{12}} \end{Bmatrix} \tag{47}$$

or

$$\mathbf{D\ q} = \omega^2\ \mathbf{M\ q} \tag{48}$$

where **D** is an un-symmetric matrix . Multiplying both sides with $\mathbf{D^T}$, we get

$$\mathbf{D^T\ D\ q} = \omega^2\ \mathbf{D^T\ m\ q} \tag{49}$$

Or

$$\mathbf{G\ q} = \omega^2\ \mathbf{E\ q} \tag{50}$$

5.1 Equilibrium and continuity conditions at the internal nodes

5.1.1 Equilibrium at internal nodes

Since the beam is divided into *ne* = twelve elements, there will be ((*ne*-1) = 11) eleven internal nodes. The axial force *P* of the 11th sampling point of the first element is equal to the value of the first sampling point of the second element. Establishing the equilibrium for *P* at the first internal node, we get

$$P(1{,}11) - P(2{,}1) = 0 \tag{51}$$

Introducing these as constraints in Eq. 51 the additional constraint equations can be written as

$$G1(1{,}11) = 1; \quad G1(1{,}67) = -1 \tag{52}$$

Similarly equilibrium for P can be established for all the ne-1 (11 internal) nodes. Equilibrium equations can be established for V at the first internal node as

$$G1(12{,}22) = 1; \; G1(12{,}78) = -1 \tag{53}$$

Hence equilibrium for M can be established for all the *(ne*-1 = 11) eleven internal nodes.
and similarly these equations are written at other ten internal nodes**.**

5.1.2 Compatibility at the internal nodes

The rotation about x axis of the 11th sampling point of the first element is equal to the rotation of the first sampling point of the second element which is given as

$$\psi(1{,}11) = \psi(2{,}1) = 0 \tag{54}$$

or

$$G1(34{,}33) = 1; \quad G1(34{,}100) = -1 \tag{55}$$

Now compatibility equations are established at other ten points.
Similarly compatibility equation can be established for v and w.
The equilibrium and compatibility at the internal nodes can be written as

$$\underset{66\times 792}{\mathbf{G}_1} \quad \underset{792\times 1}{\mathbf{q}} = \underset{66\times 1}{\mathbf{0}} \tag{56}$$

5.1.3 Boundary conditions at the domain ends

Since it is the system of six first order differential equations, six boundary conditions are necessary to solve the problem. The boundary conditions $[\mathrm{G}]_2\{\mathrm{r}\} = \{0\}$ must be added as constraints to Eq. 56.

Clamped – Clamped

Left support Clamped

$$\psi(\alpha=\phi_L)=0;\; G2(1{,}34)=1;\;\; v(\alpha=\phi_L)=0;\;\; G2(2{,}45)=1;\;\; w(\alpha=\phi_L)=0,\; G2(3{,}56)=1 \tag{57}$$

Right support Clamped

$$\psi(\alpha=\phi_R)=0;\; G2(4{,}770)=1;\; v(\alpha=\phi_R)=0;\; G2(5{,}781)=1;\; w(\alpha=\phi_R)=0,\; G2(6{,}792)=1 \tag{58}$$

where 'α' is the angular coordinate along the length of the arch girder.

Hinged – Hinged support

Left support Hinged

$$M(\alpha=\phi_L)=0;\; G2(1{,}23)=1;\;\; v(\alpha=\phi_L)=0;\;\; G2(2{,}45)=1;\;\; w(\alpha=\phi_L)=0,\; G2(3{,}56)=1 \tag{59}$$

Right support Hinged

$$M(\alpha=\phi_R)=0;\; G2(4{,}759)=1;\; v(\alpha=\phi_R)=0;\; G2(5{,}781)=1;\; w(\alpha=\phi_R)=0,\; G2(6{,}792)=1 \tag{60}$$

For numbering scheme see Fig. 3.

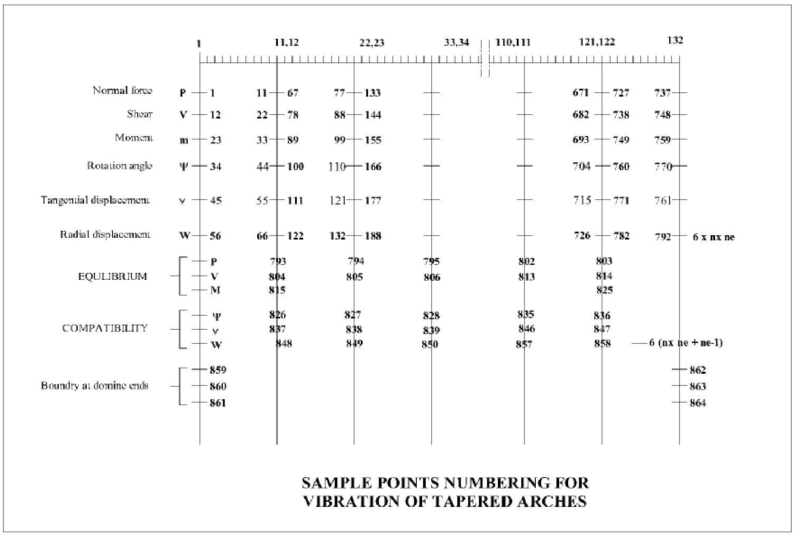

Fig. 3 Sample points numbering for vibration of tapered arches

The above boundary conditions are written in matrix form as

$$[G]_2\{q\} = \{0\} \tag{61}$$

Incorporating the equilibrium and compatibility conditions at the internal nodes as well as boundary conditions and using Wilson's Lagrangian multiplier method (Wilson 2002), we get the resulting equation as

$$\begin{bmatrix} \mathbf{G} & \mathbf{G_1^T} & \mathbf{G_2^T} \\ \mathbf{G_1} & \mathbf{0} & \mathbf{0} \\ \mathbf{G_2} & \mathbf{0} & \mathbf{0} \end{bmatrix} \begin{Bmatrix} \mathbf{q} \\ \boldsymbol{\lambda}_1 \\ \boldsymbol{\lambda}_2 \end{Bmatrix} = \omega^2 \begin{bmatrix} \mathbf{E} & \mathbf{0} & \mathbf{0} \\ \mathbf{0} & \mathbf{0} & \mathbf{0} \\ \mathbf{0} & \mathbf{0} & \mathbf{0} \end{bmatrix} \begin{Bmatrix} \mathbf{q} \\ \boldsymbol{\lambda}_1 \\ \boldsymbol{\lambda}_2 \end{Bmatrix} \tag{62}$$

where $\mathbf{G_1}\ \mathbf{q} = \mathbf{0};\ \mathbf{G_2}\ \mathbf{q} = \mathbf{0}$ denote the boundary constraints at internal and boundary nodes and $\boldsymbol{\lambda}_1, \boldsymbol{\lambda}_2$ are the Lagrangian multipliers.

The matrix on the right hand side of Eq. 62 will lead to similar to Mass matrix. When this is solved as an eigen value problem, we get natural frequencies of lateral vibration of an arch.

For the axially functionally graded material the variation of E and mass density ρ are given throughout the length of the arch and for a non-prismatic arch, variation in both Area (*A(x))* and Moment of Inertia *(I(x))* are also considered. Hence the lateral vibration of functionally graded non prismatic arch may be carried out using DQEL.

A computer program has been developed to solve any arch with variable cross section with '*ne*' elements and '*n*' sampling points and with axially functionally graded material properties.

5. Numerical examples

DEQL method is used to solve the six first order differential equations, subjected to equilibrium and compatibility of internal nodes as well as the end constraints. To show the validity of the present analysis, the lowest five dimensionless frequency parameters ($D_i = 4\omega_i\,(r\theta)^2$ $\sqrt{\mu_c / E_c I_c}$) (μ_{c-} mass per unit length at the crown) for uniform circular arches with various open angles (2θ) and different slenderness ratios $r/i = r\sqrt{A_c / I_c}$ are compared with Tufekci and Arpaci (1998) in Tables 1 and 2 for clamped-clamped and pinned-pinned end conditions and good agreement is obtained. The numerical results of clamped clamped circular arch of uniform cross section are compared with the results obtained by Irie *et al.* (1983) in Table 3 and very good agreement is observed. Tables 4 and 5 give the lowest four frequency parameters for the circular arches (depth, width and square taper) with clamped-clamped and hinged-hinged end constraints. From these results, it is clear that C_i values increase as the value of n increases with exception for hinged-hinged arches with width taper. There is an increase in C_i values when "*S*" increases. C_i values for fixed - fixed end constraints are more than that for hinged – hinged end constraints, In Table 6, the values of C_i are presented for parabolic, catenary, elliptic and sinusoidal arches for various values of '(f'= h/s)', '*S*' and '*n*'. These values are compared with Oh *et al.* (1998b) and these values agree within 3% of Oh's values except for three cases.

Fig. 4 shows the effect of '$f = h/s$' on frequency parameter for a circular, parabolic, catenary, elliptic and sinusoidal arches for S = 200 and n = 2 for depth tapered. For elliptic and sinusoidal arches β = 0.5 is assumed. From the figure, it is clear that the arch geometry has very little effect on the frequency parameter and the same conclusion is arrived by Oh *et al*. (2000). In Fig. 4 the cross over point represents two coincidence natural frequencies, one corresponding to symmetric mode and the other corresponding to anti-symmetric mode. When the end conditions change from pinned – pinned to clamped –clamped, C_i values increase. When 'f' becomes very small, the arch approaches to straight beam and C_i approaches to values for straight beam.

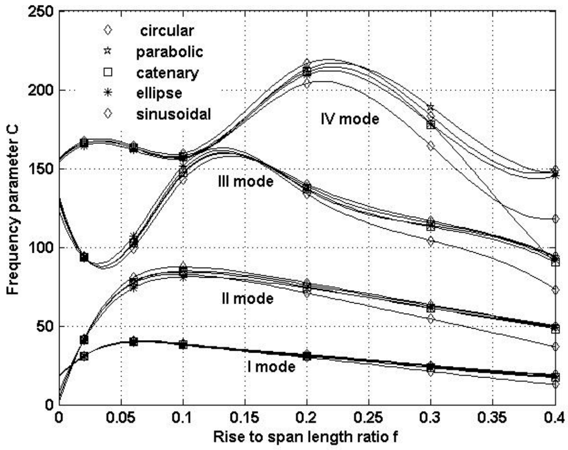

Fig. 4 Effect of f on C for hinged hinged arch depth taper (S = 200, n = 2)

Table 1 Frequency coefficient D_i = $4\omega_i\,(r\theta)^2\sqrt{\mu_c / E_c I_c}$ for uniform fixed-fixed circular arches for various open angles and various slenderness ratios $r\sqrt{A_c / I_c}$ Ref . (Tufekci and Arpaci 1998)

Open angle	Slenderness ratio	source	Mode				
			1	2	3	4	5
90deg	100	DQEL	55.3506	102.4188	188.5771	219.2464	299.3354
		Ref *	55.3434	102.3868	188.4994	219.1514	299.1958
	75	DQEL	54.9935	98.5633	174.9941	185.2423	285.0016
		Ref *	55.9768	98.5094	174.9116	185.1081	284.7500
	50	DQEL	54.0083	86.2719	132.8349	176.1028	266.3199
		Ref *	53.9660	86.1908	132.7272	175.8392	265.8141
120deg	100	DQEL	51.7159	101.9612	185.7791	269.3074	393.9432
		Ref *	51.7045	101.9366	185.7236	269.2141	393.7767
	75	DQEL	51.5145	100.6821	183.8166	253.6826	332.5862
		Ref *	51.5012	100.6416	183.7216	253.5605	332.4988
	50	DQEL	50.9643	96.9342	178.3952	198.1263	283.2889
		Ref *	50.9332	96.8517	178.1998	198.0489	282.9555
150deg	100	DQEL	47.5082	98.8818	181.2495	271.6077	392.0931
		Ref *	47.5326	98.8691	181.2108	271.5375	391.9823
	75	DQEL	47.4159	98.2470	179.9788	267.0457	286.5363
		Ref *	47.4091	98.2165	179.9086	266.9185	386.3414
	50	DQEL	47.0841	96.4355	176.4357	250.2842	339.1054
		Ref *	47.0612	96.3684	171.2864	250.0629	338.9705
180deg	100	DQEL	43.2099	94.7754	175.7434	268.5460	387.8478
		Ref *	43.1709	94.7557	175.7111	268.4875	387.7377
	75	DQEL	43.1173	94.3942	174.8677	266.0814	384.0414
		Ref *	43.0922	94.3658	174.8113	265.9794	383.9120
	50	DQEL	42.8881	93.3234	172.4165	258.6965	373.1201
		Ref *	42.8697	93.2681	172.2951	258.4766	372.7893

Fig. 5 shows the effect of 'S' on C_i values for parabolic hinged – clamped condition (f = 0.2, n = 2, breadth taper). As 'S' increases, the frequency parameter C_i for all the four modes increase other parameters remaining constant. When 'S' increases to 200, C_i values approach horizontal asymptotes. It can be observed that when the frequency curve is horizontal the vibration mode is purely flexural as in straight beams.

Fig. 6 shows the effect of 'n' on C for catenary arch (square taper- S = 200, f = 0.3) for clamped-clamped condition. As the section ratio increases by increasing I_s the C_i values also increase. In the case of pinned-pinned or clamped-clamped conditions, the mode shapes show alternating pattern behaviour symmetric to anti-symmetric mode shapes as i increases from 1 to 4. The mode shapes for pinned pinned condition is shown in Fig. 7. But for pinned-clamped condition, the mode shapes are asymmetric as shown in Fig. 8.

Table 7 shows the effect of material parameter η on frequency parameter C_i for pined-clamped all types of arches for f = 0.3, S = 200, n = 5 for square taper and it is found that 'η' does not affect C_i values for all modes except the third mode.

Table 2 Frequency coefficient $D_i = 4\omega\,(r\theta)^2\sqrt{\mu_c / E_c I_c}$ for uniform pinned – pinned circular arches for various open angles and various slenderness ratios $r\sqrt{A_c / I_c}$ Ref. (Tufekci and Arpaci 1998)

Open angle	Slenderness ratio	source	Mode 1	Mode 2	Mode 3	Mode 4	Mode 5
90deg	100	DQEL	33.8352	78.7547	150.0819	214.9579	259.7254
		Ref *	33.8341	78.7259	150.0300	214.8133	259.7674
	75	DQEL	33.7441	77.7568	148.5119	173.9816	239.4179
		Ref *	33.7367	77.7025	148.4183	173.9414	239.3448
	50	DQEL	33.4876	74.4646	121.4085	144.2310	226.6233
		Ref *	33.4632	74.3412	121.4958	144.0231	226.3381
120deg	100	DQEL	30.3368	76.2604	146.9712	230.0684	339.2957
		Ref *	30.3178	76.2373	146.9290	229.9762	339.1900
	75	DQEL	30.2707	75.8775	146.0726	225.4805	321.8775
		Ref *	30.2665	75.8395	145.9973	225.3067	321.9759
	50	DQEL	30.1411	74.7733	143.5631	197.4021	242.3411
		Ref *	30.1212	74.6949	143.4124	197.2452	242.4045
150deg	100	DQEL	26.2465	72.5617	142.6226	228.0018	336.5829
		Ref *	26.4079	72.5587	142.5925	227.9351	336.4950
	75	DQEL	26.4371	72.3835	142.0619	226.1538	333.5652
		Ref *	26.3787	72.3473	141.9974	226.0291	333.3854
	50	DQEL	26.3109	71.8039	140.4470	220.2446	324.9149
		Ref *	26.2958	71.7477	140.3306	219.9901	324.5391
180deg	100	DQEL	22.5794	68.1904	137.4585	223.7963	332.1591
		Ref *	22.3497	68.1644	137.4288	223.7427	332.0705
	75	DQEL	22.4512	68.0651	137.0732	222.6863	330.0758
		Ref *	22.3325	68.0360	137.0236	222.5925	329.9577
	50	DQEL	22.3038	67.7221	135.9908	219.4897	324.2214
		Ref *	22.2836	67.6722	135.8837	219.2887	323.9065

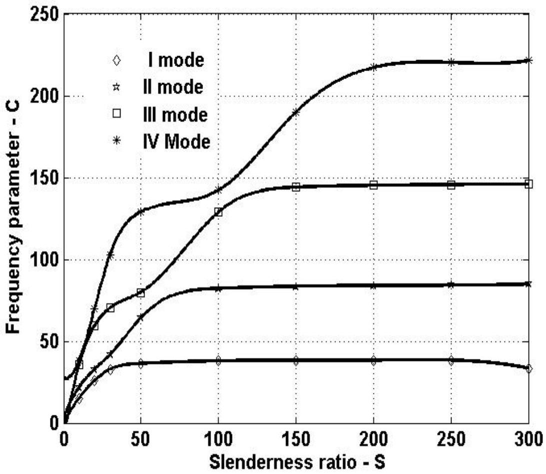

Fig. 5 Effect of S on frequency parameter C for breadth taper parabolic arch (hinged –clamped) f = 0.2, n = 2

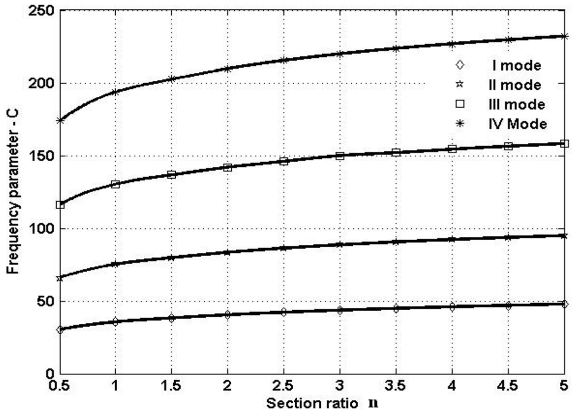

Fig. 6 Effect of n on C for catenary arch square taper Clamped – clamped (f = 0.3, S = 200)

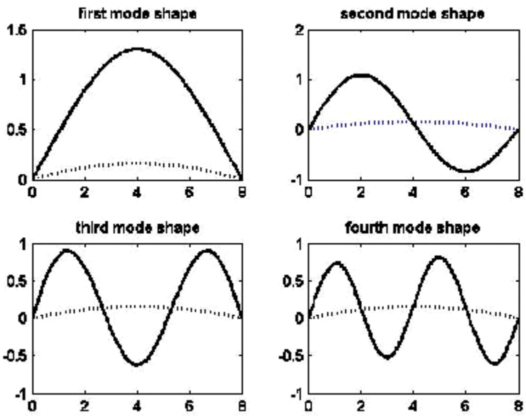

Fig. 7 Mode shapes for Sinusoidal arch S = 200, n = 1, f = 0.2 (pinned-pinned condition)

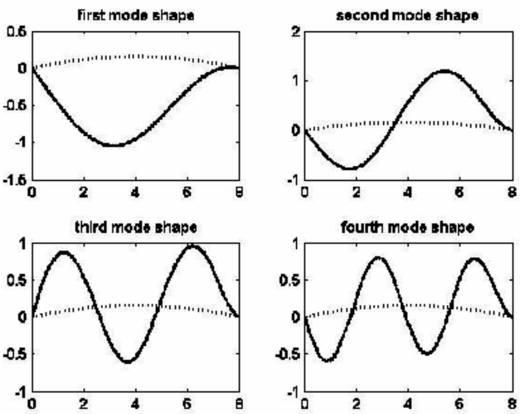

Fig. 8 Mode shapes for Sinusoidal arch S = 200, n = 1, f = 0.2 (pinned-clamped condition)

Table 3 Comparison of frequency parameter C_i between this study and Irie *et al*. (1983) (uniform section, clamped-clamped circular arch, ($\mu = kG/E = 0.327$; S = s/$\sqrt{I_c / A_c}$)

i	*h/s* = 0.134 (open angle = 60 deg)				*h/s* = 0.289 (open angle = 120deg)			
	S = 20		*S* = 100		*S*=34.64		*S* = 173.2	
	DQEL	**Irie *et al* (1983)**	DQEL	**Irie *et al* (1983)**	DQEL	**Irie *et al.* (1983)**	DQEL	**Irie *et al.* (1983)**
1	23.7215	23.70	52.7906	52.78	31.7874	31.77	35.3847	35.37
2	38.7111	38.73	75.9370	75.98	45.4941	45.51	69.7619	69.72
3	62.7664	62.35	117.7839	117.8	73.9706	73.89	127.1112	127.1
4	69.9650	69.97	170.8174	170.80	91.3690	91.14	184.2340	184.2

Table 4a Frequency parameter C_i for clamped – clamped circular arch $\mu = 0.3$. The values in brackets are obtained by Oh *et al.* (1998a) (n = 1 uniform)

h/s	*S*	*n*	Taper	*i* = 1	*i* = 2	*i* = 3	*i* = 4
0.1 open angle (45.24deg)	20	1	depth	21.7762 *(22.12)*	40.2959 *(41.59)*	62.9085 *(63.52)*	70.6604 *(74.34)*
		3	depth	24.8110 *(25.24)*	44.5429 *(45.31)*	67.0398 *(67.67)*	74.9214 *(78.57)*
		7	depth	26.5615 *(27.02)*	47.0072 *(48.41)*	69.2411 *(69.9)*	77.1815 *(81.12)*
		3	width	25.5555 *(26.06)*	45.6119 *(47.18)*	74.8959 *(75.45)*	107.4913 *(79.44)*
		7	width	27.7202 *(28.31)*	49.2189 *(50.99)*	80.0239 *(81.39)*	80.8236 *(79.44)*
		3	square	25.0259 *(25.58)*	44.9962 *(46.33)*	68.9962 *(69.6)*	75.2430 *(78.8)*
		7	square	26.9189 *(27.42)*	47.7816 *(49.28)*	72.1894 *(72.82)*	78.3781 *(82.04)*
	100	1	depth	55.9219 *(56.13)*	63.9988 *(64.16)*	115.3330 *(116.2)*	(178.3227 *(180.7)*
		3	depth	66.1409 *(66.45)*	67.5222 *(67.70)*	130.1497 *(131.4)*	200.3558 *(203.5)*
		7	depth	69.1921 *(69.39)*	72.8309 *(73.21)*	140.1217 *(141.6)*	214.2075 *(217.8)*
		3	width	63.0303 *(63.3)*	71.2110 *(71.4)*	122.0385 *(123.1)*	187.8377 *(190.5)*
		7	width	68.6244 *(68.95)*	(74.0416 *(74.25)*	129.0960 *(130.3)*	197.1211 *(200.1)*
		3	square	65.3866 *(65.69)*	68.5082 *(68.69)*	128.1852 *(129.4)*	197.3538 *(200.4)*
		7	square	70.5522 *(70.75)*	71.8382 *(72.21)*	137.5384 *(138.9)*	210.2860 *(213.8)*

Fig. 9 shows the effect of material parameters 'η' on the frequency parameter C_i for clamped-clamped elliptic arch f = 0.3, S = 200, n = 5 for all the tapers. From the figure, it is clear that 'η' does not affect C_i values for all modes except third mode. Table 8 shows the comparison of results by DQEL with the computer and experimental results of Oh *et al.* (2000) for parabolic arches with breadth taper f = 0.25, S = 200, n = 1.5 and the results agree with the computed results of Oh *et al.* (2000).

Table 5 Frequency parameter C_i for pinned – pinned circular arch μ = 0.3. The values in brackets are obtained by Oh *et al*. (1998a)

h/s	*S*	*n*	Taper	i = 1	i = 2	i = 3	i = 4
0.1	20	1	depth	16.1093	30.4204	61.6317	62.7207
				(16.44)	*(31.91)*	*(63.23)*	*(66.09)*
		3		16.4919	32.0794	64.5482	66.7691
				(17.05)	*(34.29)*	*(67.31)*	*(70.12)*
		7		16.6038	32.4347	65.2389	68.9073
				(17.37)	*(35.43)*	*(69.5)*	*(72.4)*
0.1	100	3	width	35.5621	70.9962	85.9134	144.2158
				(35.71)	*(71.21)*	*(86.58)*	*(146.3)*
		7		35.1971	73.9874	83.7505	143.9784
				(35.37)	*(74.21)*	*(84.54)*	*(146.2)*
0.1	100	3	square	37.7643	68.4839	92.1131	153.7656
				(37.94)	*(68.67)*	*(92.98)*	*(156.3)*
		7		38.3653	70.5352	93.0346	157.7529
				(38.59)	*(70.73)*	*(94.1451)*	*(160.7)*
0.25	20	1	depth	20.6117	27.8863	49.3909	59.6201
				(21.21)	*(28.31)*	*(52.31)*	*(61.06)*
		3		22.2604	29.0444	51.7835	63.6595
				(23.29)	*(29.73)*	*(55.71)*	*(65.13)*
		7		22.8835	29.5734	52.6758	66.7777
				(24.46)	*(30.58)*	*(57.92)*	*(67.82)*
0.4	20	3	width	12.4125	30.2157	40.2268	54.2474
				(12.74)	*(31.01)*	*(42.11)*	*(57.0)*
		7		12.5305	32.9200	38.2656	56.2573
				(13.03)	*(34.71)*	*(39.62)*	*(60.26)*
0.4	100	3	square	13.9122	39.2739	76.6482	121.7756
				(13.91)	*(39.36)*	*(77.14)*	*(123)*
		7		15.2774	43.9892	84.2610	133.4769
				(15.29)	*(44.16)*	*(84.97)*	*(135.2)*

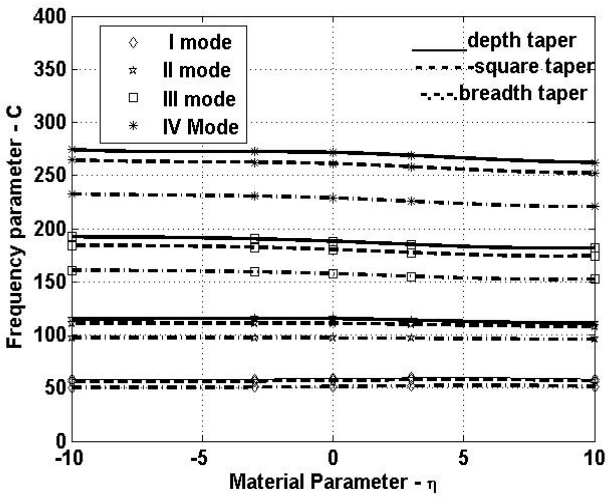

Fig. 9 Effect of *npr* on *C* (clmped-clamped) elliptic arch f = 0.3,S = 200,n = 5 for all taper

Table 6 Comparison of Frequency parameter C between current study with Oh *et al*. (1998a, 2000)

Geometry of the arch	C_i		
	This study	Oh *et al* (1998a, 2000)	%error
Parabolic hinged – hinged breadth taper s = 8m, f = 0.1, S = 50, n = 2, h = 0.8, I_c = 0.0256, A_c = 1	34.9944	36.21	3.46
	37.1970	37.16	0.08
	78.3940	82.61	5.49
	133.2718	144.6	8.27
Catenary hinged- clamped depth taper s = 8m, f = 0.2, S = 100, n = 3, h =1.6, I_c = 0.0064, A_c = 1	42,6006	43.0	0.93
	88.3354	88.8	0.529
	129.5601	129.9	0.3
	158.4535	162.3	2.369
Elliptic arch β = 0.5, s = 8m, clamped-clamped square taper f = 0.3, S = 50, n = 4, h = 2.4, I_c = 0.0256, A_c = 1	42.8659	43.63	1.74
	76.5742	77.16	0.76
	89.8305	95.06	5.62
	130.7671	145.6	10.18
Sinusoidal arch β = 0.5, s = 8m clamped-clamped, uniform, f = 0.1, S = 100, n = 1, I_c = 0.0064, A_c = 1	56.0862	56.25	0.29
	66.0381	66.25	0.319
	113.4105	114.9	1.3
	179.2729	181.7	1.34

Table 7 Effect of material parameter on frequency parameter C_i for pinned-clamped arch f = 0.3, S = 200 n = 5 square taper

η	Arch type	C_1	C_2	C_3	C_4
	circular	38.1602	84.6434	149.4412	221.8170
	parabolic	41.1833	94.2106	164.3659	246.0834
-10	catenary	40.3757	92.3759	160.8593	240.9295
	elliptic	40.5458	92.7907	161.6003	241.7517
	sinusoidal	41.6820	95.0831	166.3877	249.2921
	circular	38.0858	85.3186	148.0292	220.3857
	parabolic	40.8932	93.7539	162.8205	243.6533
-3	catenary	40.1389	92.2993	159.3430	238.6865
	elliptic	40.2966	92.6168	160.0655	239.4613
	sinusoidal	41.3634	94.4125	164./8454	246.7753
	circular	37.6917	84.1211	145.4519	218.2577
	parabolic	40.3862	92.9605	160.5721	241.2290
0	catenary	38.6894	91.4914	157.0154	236.2234
	elliptic	39.8323	91.8138	157.7486	237.0499
	sinusoidal	40.8214	93.6124	162.6504	244.3452
	circular	36.7483	81.0916	141.1559	213.3479
	parabolic	39.6326	91.4951	156.9953	236.8526
3	catenary	38.9506	89.6458	153.1950	231.5332
	elliptic	39.0825	90.0516	153.9752	232.4673
	sinusoidal	40.0537	92.3402	159.2354	240.1634
	circular	34.9134	76.4228	135.6479	205.1064
	parabolic	38.4447	88.7150	151.7375	229.3490
10	catenary	37.6194	86.1732	147.8294	223.9162
	elliptic	37.7614	86.6913	148.6107	224.8305
	sinusoidal	38.9649	90.0240	154.0840	232.8108

Table 8 Comparison of computed and experimental results of Oh *et al*. (2000) (parabolic, breadth taper, f = 0.25, S = 200, n = 1.5)

End constraint	Mode	Theory			Frequency Expt (Oh *et al.*(2000)
		C- This analysis	Frequency This analysis	Frequency Oh *et al.*(2000)	
Hinged-Hinged	1	25.4096	298.029	311.4	297
	2	63.4555	744.269	757.2	684
	3	115.7202	1357.28	1371.0	1100
	4	181.2166	2125.489	2142.0	2049
Hinged-clamped	1	33.1993	389.395	393.1	364
	2	75.2611	882.737	884.2	777
	3	131.3467	1540.565	1545.0	1215
	4	199.3177	2337.79	2350.0	2121
Clamped-Clamped	1	43.1802	506.46	494.5	460
	2	87.8069	1029.88	1020.0	916
	3	148.0646	1736.65	1733.0	1555
	4	217.5466	2551.60	2557.0	2290

(Experiment arch s = 34.64cm, h = 8.66cm, depth = 0.6cm throughout b = 2cm at crown and 3cm at the support $E = 6389 \times 10^{10}$, γ = 2680kg/m^3)

6. Conclusions

For a uniform circular arch with clamped-clamped or pinned-pinned ends, frequency values increase as opening angle decreases for constant slenderness ratio. For the same opening angle, as slenderness ratio decreases in general, five frequency parameters also decrease. This observation is in line with Tufekci and Arpaci (1998). It is also seen that as the taper ratio increases the frequency parameter values also increase as observed by Oh *et al*. (1998a). The frequency parameters for various geometry arches with different boundary conditions agree with the values obtained by Oh *et al*. (1998a, 2000). The material parameter η – does not have significant effect on the frequency parameter for (pinned – clamped boundary condition) all types of arches (f = 0.3, S = 200, n = 5) for square taper except the third mode. It is also seen that the material parameter η does not affect frequency parameter for clamped – clamped elliptic arch (f = 0.3, S = 200, n = 5) for all types of tapers.

Regarding the numerical technique DQEL, the following conclusions are arrived at.

DQEL can capture the effect of variable cross section and the material non-homogeneous parameter due to axially graded material. It is easy to incorporate boundary condition in this method. This does not need the construction of an admissible function that satisfies boundary condition a priori. Since the governing equation is written in terms of four first order differential equations, it is much easier to consider the weight coefficients based on Lagrangian interpolation technique for the first order derivative of the variable. In DQEL it is an easy task to incorporate different geometries of arches, material properties, cross sectional properties of the arch. It is also explained how Lagrangian multiplier method is used to convert rectangular matrix to square matrix by incorporating boundary condition using Wilson's method.

Acknowledgements

The author thanks the management and principal Dr. R. Rudramoorthy of PSG College of Technology, for giving necessary facilities to complete the work described in this paper. The author would like to express his gratitude to the anonymous reviewers for their constructive comments towards enhancing the paper quality. The author also thanks Prof. B.K. Lee of Wonkwang University, South Korea for his encouragement and advice and also for giving permission to the author to use the results of his research findings for comparison with the present research.

References

Bellman, R. and Casti, J. (1971), “Differential quadrature and Long term Integration”, *J. Math. Anal. Appl*., **34**, 235-238.

Bert, C.W., Wang, X. and Striz, A.G. (1993), “Differential quadrature for static and free vibration analysis of anisotropic plates”, *Int. J. Solids. Struct*., **30**(13), 1737-1744.

Bert, C.W., Wang, X. and Striz, A.G. (1994), “Static and free vibration analysis of beams and plates by differential quadrature method”, *Acta. Mech*., **102**, 11-24.

Borg, S.F. and Gennaro, J.J. (1959), *Advanced Structural Analysis*, Van Nostrand, Princeton, NJ.

Boresi, A.P., Sidebottom, O.M., Seely, F.B. and Smith, J.O, (1978), *Advanced Mechanics of Materials,* John Wiley and sons, New York.

Chidamparam, P. and Leissa, A.W. (1993), “Vibration of planar curved beams, rings and arches”, *Appl. Mech. Rev*., **46** (9), 467-483.

Den Hartog, J.P. (1928), “The lowest natural frequencies of circular arcs”, *Philos. Mag*., **75**, 400-408.

Friedman, Z. and Kosmatka, J.B, (1998), “An accurate two-node Finite Element for shear deformable curved beams”, *Int. J. Numer. Methods Eng*, **41**,473-498.

Gupta, A.K. (1985), “Vibration of tapered beams”, *J. Struct. Eng., ASCE*, **111**,19-36.

Gutierrez, R.H., Laura, P.A.A., Rossi, R.E., Bertero, R. and Villaggi, A. (1989), “In-plane vibrations of non-circular arcs of non-uniform cross-section”, *J. Sound. Vib*, **129**, 181-200.

Henrych, J. (1989), *The dynamics of arches and frames,* Elsevier, New York.

Huang, C.S., Tseng, Y.P., Leissa, A.W. and Nieh, A.Y. (1998), “An exact solution for in plane vibrations of an arch having variable curvature and cross section”, *Int. J. Mech. Sci.*, **40**(11), 1159-1173.

Irie, T., Yamada, G. and Tanaka, K. (1983), “Natural frequencies of in-plane vibration of arcs”, *J. Appl. Mech*., **50**(2), 449-452.

Kang, K., Bert, C.W. and Striz, A.G. (1995), “Vibration analysis of shear deformable circular arches by differential quadrature method”, *J. Sound. Vib*., **183**, 353-360.

Kawakami, M., Sakiyama, T., Matsuda, H. and Morita, C. (1995), “In-plane and out-of-plane free vibrations of curved beams with variable sections”, *J. Sound Vib*., **187**, 381-401.

Kim, J.G. and Lee, J.K. (2008), “Free vibration Analysis of arches based on the hybrid mixed formulation with consistent quadratic stress functions”, *Comput. Struct*., **86**(15-16), 1672-1681.

Koizumi, M. (1993), “The concept of FGM”, *Ceram. Trans*, *Functionally Graded Materials*, **34**, 3-10.

Koizumi, M. (1997), “FGM activities in Japan”, *Composites: part B*, **28**,1-4.

Laura, P.A.A., Verniere De Irassar, P.L., Carnicer, R. and Bertero, R. (1988), “A Note on vibrations of a circumferential arch with thickness varying in a discontinuous fashion”, *J. Sound. Vib*., **120,** 95-105

Lawrence, J.D. (1972), *A Catalog of special plane curves*, Dover publishers.

Lee, B.K. and Wilson, J.F. (1989), “Free vibration of arches with variable curvature”, *J. Sound Vib*., **136**, 75-89.

Leontovich, V. (1959), *Frames and Arches*, Mc-Graw-Hill.

Lockwood, E.H. (1961), *A book of curves*, Cambridge University Press.
Malekzadeh, P. (2009), "Two dimensional in-plane free vibration of functionally graded circular arches with temperature dependent properties", *Compos. Struct*., **91**(1), 38-47.
Malekzadeh, P. and Setoodeh, A.R. (2009), "DQM in-plane free vibration of laminated moderately thick circular deep arches", *Adv. Eng. Softw.*, **40**(9), 798-803.
Malekzadeh, P., Atashi, M.M. and Karami, G. (2009), "In-plane free vibration of functionally graded circular arches with temperature dependent properties under thermal environment", *J. Sound.Vib*., **326**(3-5), 837-851.
Malekzadeh, P., Golbahar, M.R. and Atashi, M.M. (2010), "Out of plane free vibration of functionally graded circular curved beams in thermal environment", *Compos. Struct*., **92**(2),541-552.
Malekzadeh, P. (2010), "Out-of-plane Free vibration Analysis of Functionally graded Circular curved beams supported on elastic foundation", *Int. J. App. Mech*, **2**(3), 635-657.
Maurizi, M.J., Rossi, R.E. and Belles, P.M. (1991), "Lowest natural frequency of clamped circular arcs of linearly tapered width", *J. Sound. Vib*,, **144**,357-361.
Maurizi, M.J., Belles, P.M., Rossi, R.E. and De Rosa, M.A. (1993), "Free vibration of a three-centred arc clamped at the ends", *J. Sound. Vib*., **161,**187-189.
Oh, S.J., Lee, B.K. and Lee, I.W. (1998a), "Free vibrations of circular arches with variable cross-section considering shear deformations and rotatory inertia", *Fifth Pacific Structural Steel Conference*, Seoul, Korea, October.
Oh, S.J., Lee. B.K., Lee, I.W. and Park, M.H. (1998b), "Free vibrations of noncircular arches considering rotatory inertia and shear deformation", *Comput. Mech*., Barcelona, Spain.
Oh, S.J., Lee, B.K. and Lee, I.W. (2000), "Free vibrations of non-circular arches with non-uniform cross-section", *Int. J. Solids. Struct*., **37**(36) , 4871-4891.
Piovan, M.T., Domini, S. and Ramirez, J.M. (2012), "In-plane and out-of-plane dynamics and buckling of functionally graded circular curved beam", *Compos. Struct.*, **94**, 3194-3206.
Rajasekaran, S. (2007), "Symbolic computation and differential quadrature method- A boon to engineering analysis", *Struct. Eng. Mech*., **27**(6), 713-739.
Rajasekaran, S. (2008), "Buckling of fully and partially embedded non-prismatic columns using differential quadrature and differential transformation methods", *Struct. Eng. Mech*., **28**(2), 221-238.
Romanelli, E. and Laura, P.A. (1972), "Fundamental frequencies of non-circular, elastic, hinged arcs", *J. Sound. Vib*., **24**, 17-22.
Schilling, R.L. and Harris, S.L. (2000), *Applied Numerical Methods for Engineers using Matlab and C*, Brooks/Cole, Thomson Learning.
Shafiee, H., Naei, M. and Eslami, M. (2006), "In-plane and out-of –plane buckling of arches made of functionally graded material", *Int. J. Mech. Sci*, **48**, 907-915.
Shahba, A., Attarnejad, R., Tavanaie Marvi, M. and Hajilar, S. (2011), "Free vibration and stability analysis of axially functionally graded tapered Timoshenko beams with classical and non-classical boundary conditions", *Composites–part–B-Eng.*, **42**(4), 801-808..
Shahba, A. and Rajasekaran, S. (2012), "Free vibration and stability of tapered Euler-Bernoulli Beam made of axially Functionally graded material", *Appl. Math. Model*., **36**, 3094-3111.
Shahba, A., Attarnejad, R., Jandaghi Semnani, S. and Honarvar Gheitanbaf, H. (2012), "New shape functions for non uniform curved Timoshenko beam with arbitrarily varying curvature using basic displacement functions", *Meccanica*, DOI, 10.1007/s 11012-012-9591-9.
Shu, C. (2000), *Differential Quadrature and its application in Engineering*, Springer, Berlin.
Tufekci, E. and Arpaci, A. (1998), "Exact Solution of in-plane vibrations of circular arches with account taken of axial extension, transverse shear and rotatory inertia effects", *J. Sound. Vib*., **209**(5), 845-856.
Tufekci, E. and Dogruer, O.Y. (2006), "Out-of-plane free vibration of a circular arch with uniform cross section: Exact solution", *J. Sound. Vib*., **291**(3-5),525-538.
Valetsos, A.S., Austin, W.J., Pereia, C.A.L. and Wung, S.J. (1972), "Free in-plane vibration of Circular Arches", *J. Eng. Mech-ASCE*., **98** (2), 311-329.
Volterra, E. and Morell, J.D. (1960), "A Note on the lowest natural frequency of elastic arcs", *J. Appl.*

Mech., **27**, 744-746.
Wang, T.M. (1975), “Effect of variable curvature on fundamental frequency of clamped parabolic arcs”, *J. Sound. Vib*., **41**,247-251.
Wilson, E.L. (2002), *Three Dimensional Static and Dynamic Analysis of Structures,* Computers and Structures Inc., Berleley, California.
Wilson, J.F., Lee, B.K. and Oh, S.J. (1994), “Free vibrations of circular arches with variable cross-section”, *Struct. Eng. Mech*, **2**(4), 345-357.
Wolf. Jr., J.A. (1971), “Natural Frequencies of Circular Arches”, *J. Struct. Eng-ASCE*., **97**(9), 2337-2350.
Yousefi, A. and Rastgoo, A. (2011), “Free vibration of functionally graded spatial curved beams”, *Compos. Struct*., **93**(11), 3048-3056.
Zhao, Y. and Kang, H. (2008), “In-plane free vibration analysis of cable-arch structure”, *J. Sound. Vib*., **312**(3), 363-379.